

SYNTHESIS AND CHARACTERIZATION OF POLYTHIOPHENE WITH POLYVINYL ALCOHOL NANOCOMPOSITES FOR ENERGY STORAGE

Arvind Kumar*¹, Deepak Kumar*², Onkar Singh Bhatia*³

*^{1,2,3}Department Of Mechanical Engineering, UIET, Universal Group Of Institute, Lalru, India.

DOI : <https://www.doi.org/10.56726/IRJMETS49105>

ABSTRACT

In this work, the oxidative chemical polymerization process was used to synthesize conducting polymer PTh and PTh/PVA nanocomposites. Research has been conducted on the optical, electrical, and electrochemical characteristics of PVA and PTh/PVA nanocomposites. Using FTIR and UV/Visible spectroscopy, the optical characteristics of PTh and PTh/PVA nanocomposites have been determined. Based on their I-V properties, PTh/PVA nanocomposites' electrical conductivity has been computed. The electrochemical performance has been studied using cyclic voltammetry.

Keywords: PTH/PVA, Optical Properties, Mechanical Properties, Supercapacitors, Chemical.

I. INTRODUCTION

In recent decades, supercapacitors, also known as electrochemical capacitors or ultracapacitors, have been used as power storage devices due to their high power density, long cycle life, and quick charge rates [1]. A supercapacitor (SC) is a type of capacitor that solves the problems with electrolytic capacitors and rechargeable batteries by having a higher capacity than regular capacitors while maintaining lower voltage limits. It can recognize and transfer charge much faster than batteries, holds 10 to many times more energy per unit volume or mass, and withstands many more cycles of charge and discharge than rechargeable batteries.

Supercapacitors are used in applications that need a lot of short charge/discharge cycles rather than long-term reduced energy storage in vehicles such as cars, trucks, trains, cranes, and lifts. They can be used for burst-mode control delivery, regenerative braking, and temporary energy stockpiling [2]. Static irregular access memory (SRAM) uses smaller units as memory reinforcement. Supercapacitors present a viable way to handle the expanding demands of commonplace energy storage applications. Supercapacitors, which may be employed in a range of applications, play a crucial place in resolving many conflicts between batteries and regular capacitors due to their larger power thickness compared to batteries and bigger vitality thickness when compared to regular capacitors [3]. Because of its low effort, easy synthesis, high putative specific capacitance, and ecological durability, PTh (poly thiophene) is one of the most concerning conductive polymers [4–8]. However, the PTh's mechanical execution and planning are typically subpar, making it ill-suited to handle a manageable amount of strain. Notably, hydrogel is a frequent, robust, and delicate substance with three-dimensional hydrophilic polymeric structures. The advantages of the guiding polymers and hydrogel can be combined with the PTh hydrogel. Because of its great versatility, PTh hydrogel has the potential to be used in flexible energy storage devices [9, 10].

However, like with most conductive polymer-based hydrogels with an elasticity of less than 1 MPa, the mechanical characteristics of PTh hydrogels are still typically poor [11]. Thus, the synthesis of PTh with remarkable mechanical properties remains an amazing test. PVA hydrogel is a type of water-soluble polymer with remarkable natural resemblance and substance solidity. PVA hydrogel in particular has excellent mechanical quality [12]. Furthermore, PVA has also been widely studied and used as a hydrogel and potent electrolyte [13]. It is widely acknowledged that techniques for accurately blending at least two different types of polymers can form composites with unique structures and enhanced capabilities. By combining PTh and PVA hydrogel, an adjustable composite may be created that enhances the mechanical capabilities of PTh. In composite, a synergistic effect might be produced. Separately, PTh hydrogel and PVA hydrogel can enhance the specific capacitance and mechanical quality of the composite. PVA hydrogel can also be used as a strong electrolyte in composite materials. Because of its exceptional mechanical qualities, the PTh/PVA composite could be used as the dynamic material for stretchy energy storage devices.

II. MATERIALS AND METHOD

2.1. Synthesis of PTh

Polythiophene (PTh) was synthesized using a traditional chemical oxidation process. A flask containing 100 ml of dichloromethane was filled with 0.5 M of thiophene monomer, and a mixture of thiophene and anhydrous $FeCl_3$ was stirred. A black precipitate was produced, and the polymerization continued for a predetermined time. The PTh was then passed through filters, washed with acetone and acetonitrile, and dried for 24 hours at $60^\circ C$ in a vacuum oven..

2.2. Synthesis of PTh/PVA nanocomposite

12 ml of DI is mixed with 1.2 g of PVA at $60^\circ C$ until a transparent, clear solution forms. To create PTh/PVA nanocomposites, sonicate 4 ml DMF with 0.4 g of PTh for one hour. The result is a transparent, viscous PTh/PVA nanocomposites solution. Platinum wire was utilized as the counter electrode and Ag/AgCl as the reference electrode for the cyclic voltage measurement. We had selected PVDF as the additive binder, PTh/PVA as the active material, and conducting carbon as the working electrode. The electrolyte used to take the C-V measurement is PVA/ H_2SO_4 . PTh/PVA, PVDF, and conductive carbon were combined in an 8:1:1 ratio to create a slurry. On FTO glass, the aforementioned combination is applied in a thin layer. On an autolab potentiostat galvanostat using Nova software, the C-V measurement is carried out at various scan rates, i.e., 0.4, 0.6, and 0.8 mV/s, and the working voltage ranges from -0.8 V to 0.2 V. Keithley source meter 2400 has been used to measure I-V.

III. RESULTS AND DISCUSSION

3.1. Optical Properties

UV/Vis absorption spectra

Figure 1 shows the UV/Vis spectra of (a) PTh, and (b), PTh/PVA. The observed absorption peaks are around 440 nm and 420 for PTh, and PTh/PVA nanocomposite, respectively. The absorption peak position attributed to the $n-\pi^*$ electronic transition of the conjugated molecules. This peak position (~ 420 nm) further confirms the longer conjugation length of the prepared polythiophenes. When PVA are distributed across the PTh matrix, there is a discernible shift in the absorption spectra. The successful interaction of PVA with the PTh polymer chain may be the cause of the red shift of the absorption transition to higher wavelengths. The straight line segment of the $(\alpha h\nu)^2$ vs. $h\nu$ graph is extrapolated to the $h\nu$ axis to determine the band gap (E_g). The plot of $(\alpha h\nu)^2$ vs. $h\nu$ is displayed in the figure 1 inset. The value of E_g for PTh and PTh/PVA nanocomposite is determined to be 3.91 eV and 4.02 eV, respectively, by projecting the graph to the $h\nu$ -axis [14].

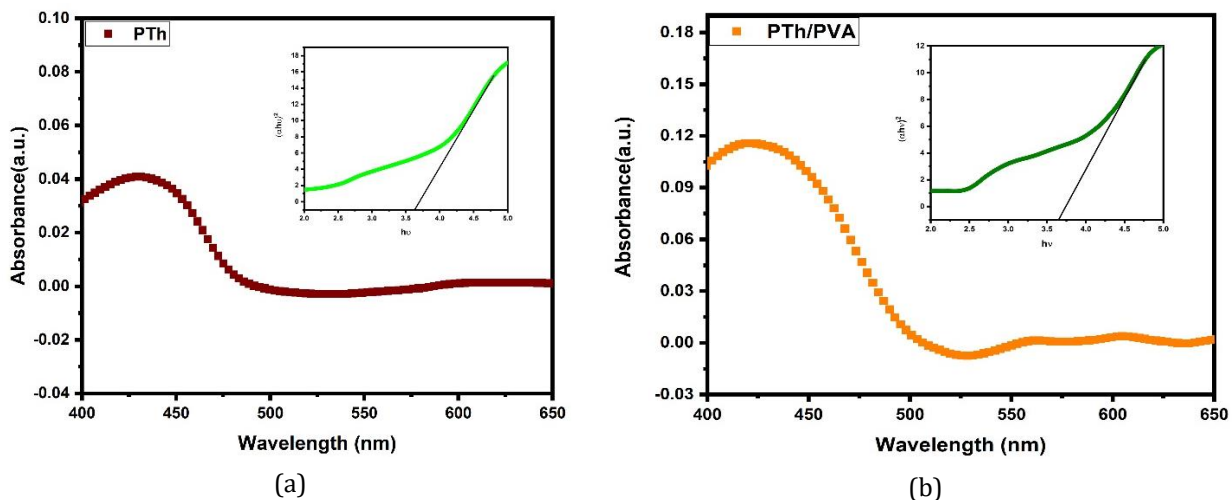


Figure 1: (a) UV/Vis Spectra of PTh and (b) PTh/PVA nanocomposite

FTIR Spectra

The type of bonding in the film material was ascertained by measuring the PTh/PVA nanocomposites' FTIR spectra. The FTIR spectra of the PTh/PVA nanocomposite and pure

PTh are displayed in Figure 2. The C=N and C=C stretching modes for the quinoid and benzenoid rings, respectively, are attributed to the peaks at $\sim 1447.82 \text{ cm}^{-1}$ and 1639 cm^{-1} (benzenoid unit) [15]. C-N and N-Q-N stretching are responsible for the observed peaks at 1179.09 cm^{-1} and 1108.42 cm^{-1} . The intensity of PTh/PVA decreases when PVA is added to the PTh matrix, indicating a positive interaction between PTh and the PTh/PVA nanocomposite.

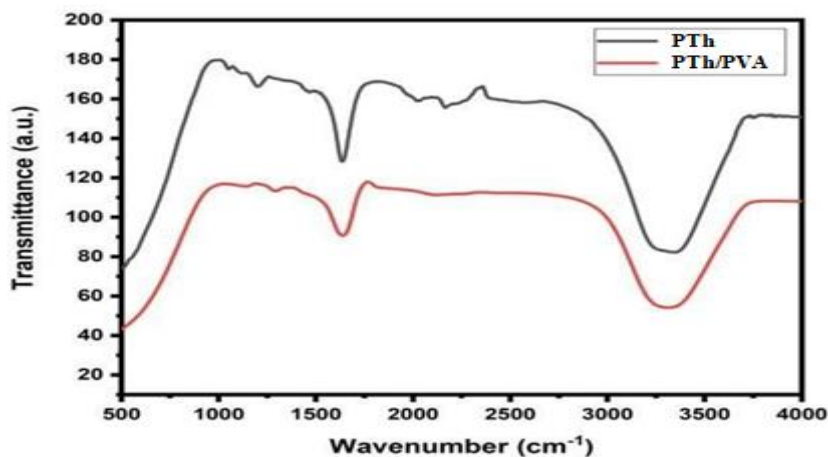


Figure 2: FTIR Spectra of PTh/PVA nanocomposite

3.2. ELECTRICAL MEASUREMENTS

Current-Voltage (I-V) measurement

The I-V properties of PTh/PVA film is displayed in Figure 3. The ohmic behaviour of these samples is indicated by their linear I-V up to the working voltage range. It is discovered that PTh/PVA nanocomposites have an electrical conductivity of $5.4 \times 10^{-2} \text{ Scm}^{-1}$, indicating that PTh is a conducting material.

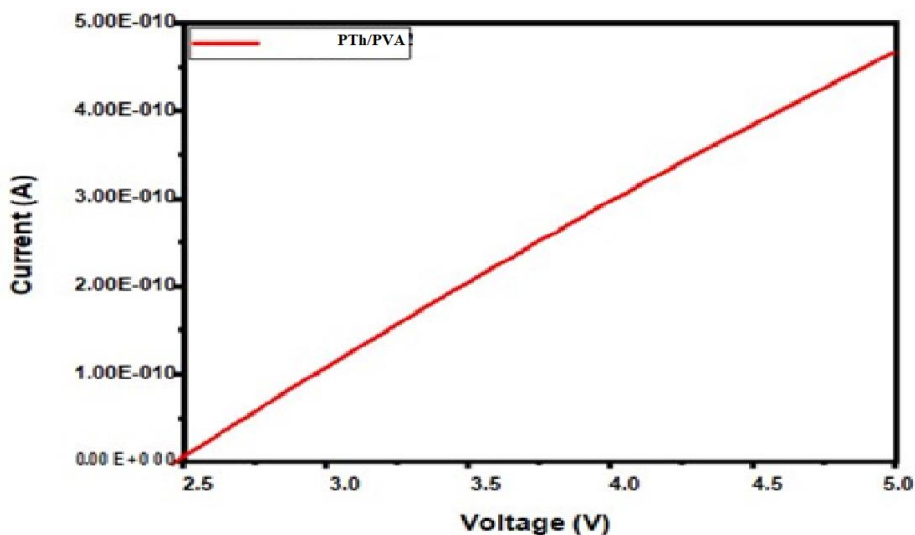


Figure 3: Current vs. voltage of PTh/PVA nanocomposite

3.3. ELECTROCHEMICAL PERFORMANCE ANALYSIS

Cyclic Voltammetry

The cyclic voltammograms of the PTh/PVA nanocomposite at various scan rates $0.4, 0.6, 0.8,$ and 1 mVs^{-1} are displayed in Figure 4(a). PTh/PVA thin film cyclic voltammograms were recorded in diluted aqueous $1 \text{ M H}_2\text{SO}_4$ over a voltage range of -0.8 to 0.2 V versus. Two pairs of redox peaks are visible to have emerged in the -0.8 to 0.2 V scan region [16,17]. The two sets of observed redox peaks correspond to the progression of PTh which suggest PTh/PVA's pseudocapacitance highlight. Furthermore, in CV, the unquestionable rise in peak flows as output rates increase demonstrates the high rate ability and responsiveness [18, 19].

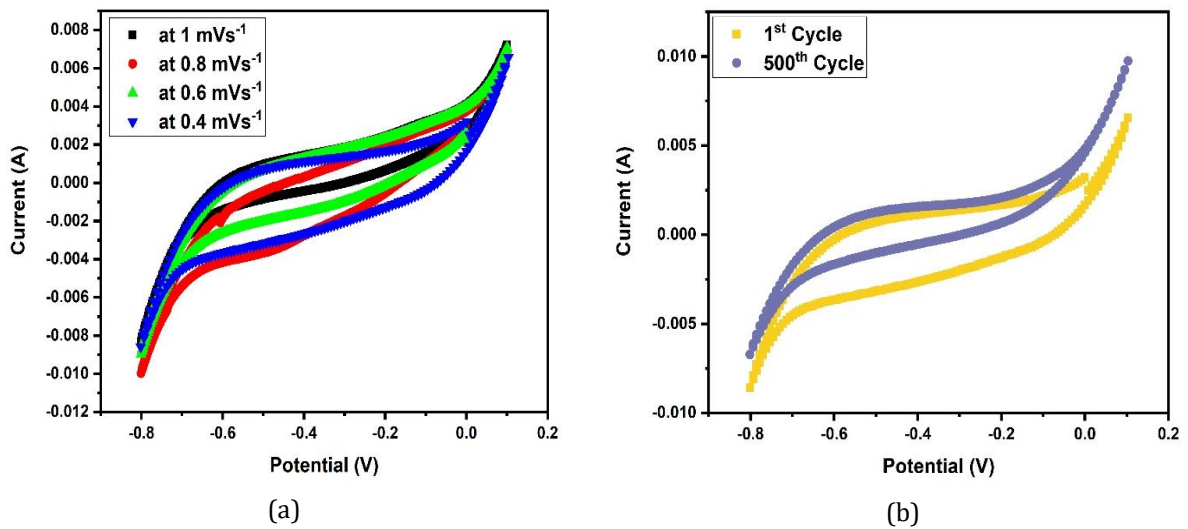


Figure 4: (a) Cyclic Voltammetry of PTh/PVA nanocomposite at different scan rate, and (b) Cyclic Voltammetry of PTh/PVA nanocomposite at 0.4 mVs⁻¹ scan rate for 1st and 500th cycle.

Table 1 displays PTh/PVA's specific capacitance at various scan rates. It is evident that PTh/PVA can achieve its maximum specific capacitance at 0.4 mVs⁻¹ scan rate, or 163 F/g, and can retain 81 percent of its capacity after 500 cycles.

Table 1: Specific capacitance of PTh/PVA nanocomposite at different scan rate

Scan rate	Specific capacitance
0.4	163
0.6	107
0.8	95
1	54

In a cyclic voltammetry test, the specific capacitance decreases as the scan rate increases. This is because an increase in the scan rate makes it harder for electrolyte ions to diffuse into the internal structure and pores of the electrode (a phenomenon known as diffusion limitation) and results in an ineffective interaction between the electrolyte and electrode materials [20]. The PTh/PVA cyclic voltammetry graph is displayed in Figure 4 (b) at a scan rate of 0.4 mVs⁻¹ for the first and 500th cycles.

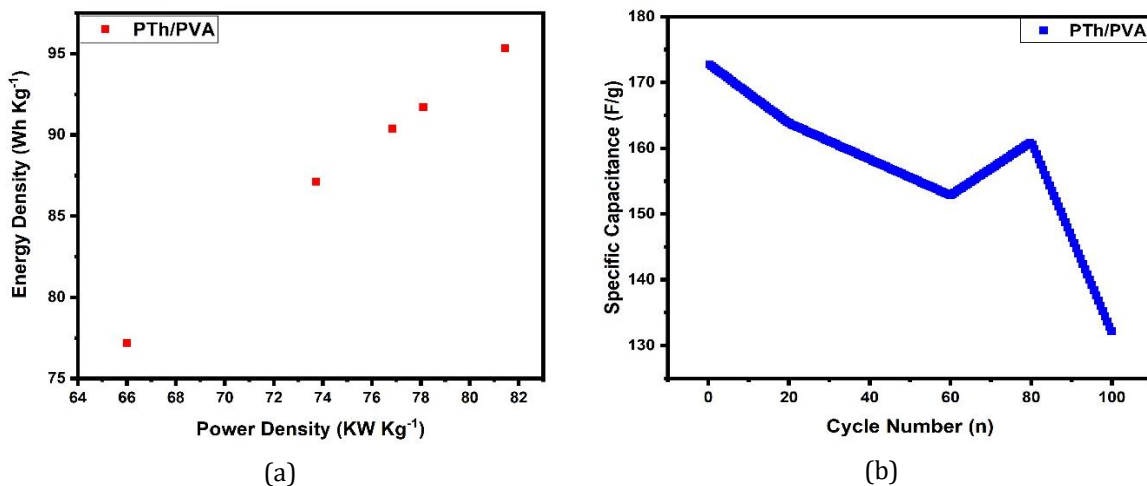


Figure 5: (a) Ragon plot of PTh/PVA nanocomposite, and (b) Variation of specific capacitance w.r.t Cycle number.

The variation in energy density and power density with respect to specific capacitance at various cycles is displayed in Table 2. It is evident that power density and energy density rise with increasing specific capacitance and fall with decreasing specific capacitance. Figure 6 (a) illustrates how energy density and power density gradually decline until cycle 300, at which point they rise once more before progressively declining again. Figure 6 (b) shows that the specific capacitance steadily falls from the first cycle to the 300th cycle, but then gradually increases from the 400th cycle onwards before decreasing again.

Table 2: Variation of Energy density and Power density w.r.t specific capacitance at different cycle number PTh/PVA nanocomposite

Cycle number	Specific capacitance (F/g)	Energy density (WhKg ⁻¹)	Power density (KWKg ⁻¹)
1	163	81.5	95.35
100	162	81.0	94.77
300	141	70.5	82.48
400	133	66.5	77.80
500	132	66.0	77.22

IV. CONCLUSION

Using the chemical oxidative polymerization approach, we have effectively synthesized PTh and PTh/PVA nanocomposite in this article. A good interaction between PVA and PTh is demonstrated using Fourier transform infrared (FTIR). Based on the UV/Vis spectra, the band gap (E_g) of these nanocomposites has been determined. The PTh/PVA nanocomposite exhibits conducting nature in its electrical conductivity. The typical cycle voltammograms of the PTh/PVA nanocomposite demonstrated the electrode's outstanding cycling stability, high specific capacitance (163 F/g), and good responsiveness and rate capability. PTh/PVA nanocomposites appear to be a viable material for supercapacitor applications based on all of these measurements.

V. REFERENCES

- [1] T. Khanikar, V. K. Singh, Opt. Mater. 88, 244-251 (2019)
- [2] Y. He, X. Wang, H. Huang, P. Zhang, Z.C. Guo, Applied Surface Science, 469, 446-455 (2019)
- [3] P. Liu, J. Yan, Z. Guangand, Y. Huang, X. Li and W. Huang, B. Gao, J. power sources 424, 108-130 (2019).
- [4] D.S. Patil, J.S. Shaikh, D.S. Dalavi, S.S. Kalagi and P.S. Patil, Mat. Chem. Phys 128, 449-455 (2011).
- [5] H. Lethe, J. Chem. Soc. 186 161-163(1862)
- [6] L. Gilchrist, J. Phys. Chem. 8 539-547(1903)
- [7] A.G. Green, A.E. Woodhead, J. Chem. Soc. Trans. 97 2388-2403(1910)
- [8] C.K. Chiang, C.R. Fincher, Y.W. Park, A.J. Heeger, H. Shirakawa, E.J. Louis, S.C. Gau, A.G. MacDiarmid, Phys. Rev. Lett. 39, 1098-1101(1977)
- [9] S. Xie, M. Gan, L. Ma, Z. Li, J. Yan, H. Yin, X. Shen, F. Xu, J. Zheng, J. Zhang, J. Hu, Electrochim. Acta 120, 408-415(2014)
- [10] S. Lee, J. Kim, S. Park, Energy 78, 298-303(2014)
- [11] M. Khalid, M.A. Tumelero, A.A. Pasa, RSC Adv. 5, 62033-62039(2015)
- [12] Y. Zhang, L. Si, B. Zhou, B. Zhao, Y. Zhu, L. Zhu, X. Jiang, Chem. Eng. J. 288, 689-700(2016)
- [13] Eftekhari, Y. Liu, P. Chen, J. Power Sources 334, 221-239(2016).
- [14] A.F. Mansour, A. Elfalaky and F.A. Maged, J. App. Phy. 7, 37-45 (2015)
- [15] P. Manivel, S. Ramakrishnan, N.K. Kothurkar, A. Balamurugan, N. Ponpandian, D. Mangalaraj, C. Vishwanathan, Mater. Res. Bull. 48, 640-645 (2013),
- [16] Olad, H. Gharekhani, Prog. Org. Coatings 81, 19-26 (2015).
- [17] Kotal M, Thakur AK, Bhowmick AK, ACS Appl Mater Interfaces 5:8374-8386 (2013).
- [18] Bhadra S, Khastgir D, Singha NK, Lee JH, Prog Polym Sci 34:783-810 (2009).
- [19] Abitbol T, Johnstone T, Quinn TM, Gray DG Soft Matter 7:2373-2379(2011).
- [20] Li M, Xue J, J Phys Chem C 118:2507-2517(2014)